PERGAMON

International Journal of Heat and Mass Transfer 43 (2000) 1591–1601

International Journal of HEAT and MASS TRANSFER

www.elsevier.com/locate/ijhmt

The effect of concentration gradient on the melting of a horizontal ice plate from above

M. Sugawara [a,*], Thomas F. Irvine [b]

[a] Department of Mechanical Engineering, Akita University, Akita 010, Japan
[b] Department of Mechanical Engineering, State University of New York at Stony Brook, Stony Brook, NY 11794, USA

Received 30 January 1998; received in revised form 30 June 1999

Abstract

The melting of a horizontal ice plate from above into a calcium chloride aqueous solution in a rectangular cavity is considered numerically and experimentally. The ice plate melts spontaneously with decreasing temperature at the melting front, even when there exists no initial temperature difference between ice and liquid. Visual observations in the liquid reveal a complicated and random natural convection mainly dominated by the concentration gradient which appears near the melting front. A very coarse and curious surface of the melting front is seen after the melting experiment, that is considered to promote the ice melting. The two-dimensional numerical model proposed in the present study predicts approximately the melting rate. © 2000 Elsevier Science Ltd. All rights reserved.

Keywords: Melting; Ice plate; $CaCl_2$ aqueous solution; Double diffusive convection

1. Introduction

The melting of ice in mixtures began as a problem for the melting of glaciers in sea water motivated by oceanographers. The melting of glaciers in sea water has become more important recently because of the increasing temperature in the earth's environment. Therefore, it is important to analyze correctly the melting rate of ice in mixtures. Some studies on melting have been previously reported. Griffin [1] analyzed the heat, mass, and momentum transfer during the melting of glacial ice in sea water. Marschall [2] presented a similarity solution for free convection on glacial ice in saline water, and computed interfacial temperatures and concentrations as a function of environmental temperatures. Huppert and Turner [3] presented experimental results for melting of an ice block in an initial saline gradient or an initial uniform salinity, and measured a series of horizontal layers with double diffusive convection. Josberger and Martin [4] investigated experimentally and analytically the melting of a vertical ice wall in salt water, and reported three different flow regimes. Carey and Gebhart [5,6] considered the melting of a vertical ice plate in saline water analytically and experimentally, and predicted the interfacial temperatures and concentrations and the velocity profiles near the melting front. Sammakia and Gebhart [7] measured the interfacial temperatures and concentrations, and velocity profiles near a vertical ice surface, and also presented visual observations of complicated flows in the salt water. Johnson and Mollendorf [8] investigated transport processes from a vertical ice surface melting in saline water, and proposed a new concept of "saline gradient dominates temperature gradient". Sugawara et al. [9] investigated the melt-

* Corresponding author.

0017-9310/00/$ - see front matter
PII: S0017-9310(99)00230-6

Nomenclature

a	thermal diffusivity, m^2/s
C	concentration, mass fraction, kg/kg
C_F	concentration at the melting front, kg/kg
c_p	specific heat, kJ/kg K
D	mass diffusion coefficient, m^2/s
g	gravitational acceleration, m/s^2
Δh	latent heat for melting, kJ/kg
H	depth of liquid layer, mm
L	length of liquid layer, mm
Le	Lewis number ($= a/D$), dimensionless
$\dot{m}_{ice}$	melting mass per unit area and time (melting rate), kg/m^2 s
M	mean melting mass per unit area, kg/m^2
p	pressure, N/m^2
S_ϕ	source term
t	time, s
T	temperature, °C or K
T_1	temperature at the bottom of ice plate (see Fig. 1), °C or K
T_2	temperature at 15 mm distance from the melting front (see Fig. 1), °C or K
T_F	temperature at the melting front, °C or K
u	x-component velocity, m/s
u_j	velocity ($u_1 = u$, $u_2 = v$), m/s
v	y-component velocity, m/s
x	horizontal coordinate
x_j	coordinate ($x_1 = x$, $x_2 = y$)
Δy_F	the most closest mesh size to the melting front, mm
y	vertical coordinate or distance from the initial melting front, mm
β_C	concentration expansion coefficient, $(kg/kg)^{-1}$
β_T	temperature expansion coefficient, K^{-1}
Γ_ϕ	general diffusion coefficient
δ	ice plate thickness, mm
ε_ϕ	convergence criterion ($\varepsilon_\phi = 10^{-5}$), Eq. (7)
λ	thermal conductivity, kJ/m s K
μ	viscosity, kg/m s
ρ	density, kg/m^3
ϕ	dependent variables (u, v, T, C)

Subscripts

F	melting front
i	initial
L	liquid
mix	mixture (aqueous solution)
P	lucite
r	reference value
S	ice

Superscript

n	iteration number, Eq. (7)

ing of a horizontal ice layer from above in sodium, calcium, magnesium chloride and urea aqueous solutions with radiative heating. Beckermann and Viskanta [10] presented numerical and experimental investigations for double-diffusive convection due to melting of a vertical ice layer in an ammonium chloride–water solution, and predicted stratified upper and uncontaminated lower regions and also predicted vertical variations of interfacial temperature and concentration. Fukusako et al. [11] reported an experimental study of the melting of a horizontal ice cylinder in saline water. Sugawara and Sasaki [12] investigated the abrupt temperature decrease in a melting system of snow experimentally and analytically. However, the transient melting and temperature decrease at the melting front have not been fully considered analytically or numerically in the above studies, even though it is important to correctly predict the melting amount for glacial ice in sea water or in some application of cold heat storage systems with change of phase.

Recently, Sugawara and Fujita [13] studied the melting of a vertical ice layer with the double effect of temperature and concentration, and presented a quantitative prediction of the melting rate and temperature depression. However, the above mentioned studies were mainly for the melting of a vertical ice plate. No studies on the melting of a horizontal ice plate, numerically and/or experimentally, have been reported.

This paper is concerned with the melting of a horizontal ice plate from above into a calcium chloride ($CaCl_2$) aqueous solution, which is considered as an extension of a previous work [13]. However, the present study reveals many new results both experimentally and analytically, that have not yet appeared in the melting of a vertical ice plate. It concerns many complicated circulations in the melt layer, which change randomly during the melting process. Moreover, a very coarse melting front was observed after all the experimental runs, which would promote the melting. A two-dimensional numerical calculation is pre-

sented to predict approximately the melting which differs by less than about 30% compared to the experimental results.

2. Analytical procedure

Fig. 1 shows the coordinate system and physical model for the melting of a horizontal ice plate. The ice plate is located below the liquid. A lucite plate is located on the top of the liquid. The environment of the melting system is assumed to be adiabatic because the test cell is surrounded by styrofoam plates as can be seen in the figure. It is assumed in the analysis that the flow in the liquid is two-dimensional, laminar and that Boussinesq approximation is considered to avoid complex calculations.

2.1. Governing equations in the liquid

Continuity

$$\frac{\partial}{\partial x_j}(\rho u_j) = 0 \tag{1}$$

Momentum, energy, mass conservation

$$\frac{\partial}{\partial t}(\rho\phi) + \frac{\partial}{\partial x_j}(\rho u_j \phi) = \frac{\partial}{\partial x_j}\left(\Gamma_\phi \frac{\partial \phi}{\partial x_j}\right) + S_\phi$$

$$S_T = 0, \qquad S_C = 0$$

$$S_u = -\frac{\partial p}{\partial x}$$

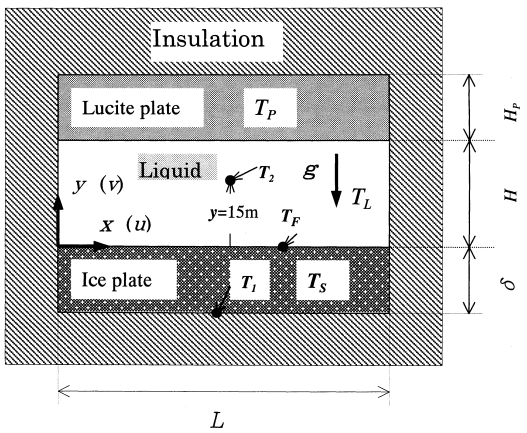

Fig. 1. Coordinate system and physical model of melting of a horizontal ice plate.

$$S_v = -\frac{\partial p}{\partial y} + \rho g \beta_T (T - T_r) + \rho g \beta_C (C - C_r)$$

$$\Gamma_{u,\,v} = \mu, \qquad \Gamma_T = \frac{\lambda}{c_p}, \qquad \Gamma_C = \rho D \tag{2}$$

where S_u and S_v include pressure gradient, and the independent variable of x_j and dependent variables of u_j and ϕ will become more clear as follows.

$$x_1 = x, \qquad x_2 = y, \qquad u_1 = u, \qquad u_2 = v$$

$$\phi = u, v, T, C$$

2.2. Governing energy equation in the ice and lucite plates

$$\frac{\partial}{\partial t}(\rho T) = \frac{\partial}{\partial x_j}\left(\frac{\lambda}{c_p}\frac{\partial T}{\partial x_j}\right) \tag{3}$$

2.3. Boundary conditions

Velocities on the interfaces between the liquid and the walls (ice, lucite, and styrofoam) are assumed to be zero. The energy balance is applied on the interface between the liquid and the lucite plate. The surrounding of the melting system is assumed to be adiabatic consistent with the experimental condition of using styrofoam plates as thermal insulation.

2.4. The heat and mass balance on the melting front

The most important boundary conditions are on the melting front since these will play a key role for the determination of the melting rate. The heat balance generally used in the classical Stefan problem is necessary as follows.

$$\text{Heat balance:} \quad \Delta h \dot{m}_{ice} = \lambda_L \left(\frac{\partial T_L}{\partial y}\right)_F - \lambda_S \left(\frac{\partial T_S}{\partial y}\right)_F \tag{4}$$

However, it is impossible to determine the melting rate by using only Eq. (4) and another important condition is needed.

$$\text{Mass balance:} \quad C_F \dot{m}_{mix} = \rho D \left(\frac{\partial C}{\partial y}\right)_F \tag{5}$$

where C_F is the concentration on the melting front, and can be assumed to be in equilibrium thermodynamically and is related to the temperature on the melting front T_F (local equilibrium assumption). How-

ever, C_F and T_F will change with time, accordingly it is impossible to pre-set C_F and T_F which causes the analysis to become difficult. Since the melting front is a semi-permeable plane for solute ($CaCl_2$), the relation of $\dot{m}_{ice} = \dot{m}_{mix}$ holds [14].

2.5. Initial conditions

Since the liquid is assumed to be static before the melting starts, u and v are zero initially. The initial temperatures of the liquid, ice, and lucite (T_{Li}, T_{Si}, and T_{Pi}) are the same, -5°C; and therefore, there exists no temperature difference between ice and liquid at the beginning of melting.

2.6. Concept of a concentration induced melting and outline of numerical procedures

For the case of no-temperature difference between ice and water initially (i.e. 0°C), it is understood that the ice does not melt due to the thermodynamic equilibrium in the melting system. On the other hand, if the initial liquid concentration and temperature are away from the liquidus line as shown in the phase diagram in Fig. 2, ice in mixtures does melt even when the both initial temperatures are in the same ($T_{Li} = T_{Si} = -5$°C seen in Fig. 2). Since it is impossible to pre-set T_F and C_F to solve the energy and conservation equations, the iterative method of SIMPLER [15] was employed in the numerical calculations. First, an unknown T_F is assumed at an approximate value near $T_{Li} = -5$°C.

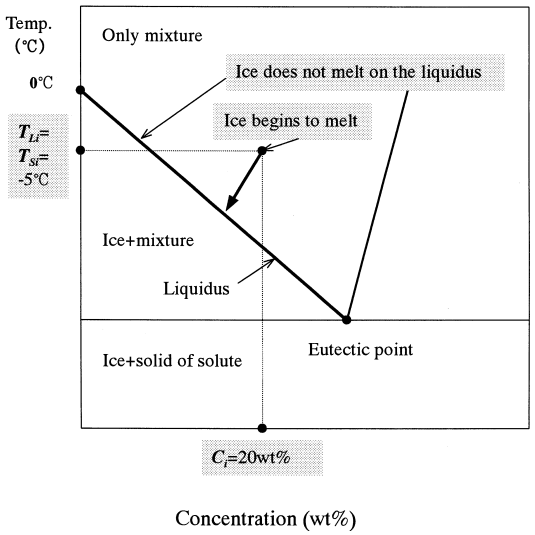

Fig. 2. Concept of a spontaneous melting of ice on the phase diagram.

Then, it is possible to calculate C_F by substituting the assumed T_F into the following equilibrium relation of T and C of the liquidus [16] for a $CaCl_2$ aqueous solution.

$$C = (3.0441 \times 10^{-3} - 2.4679T - 0.17063T^2 - 8.4228 \times 10^{-3}T^3 - 2.1251 \times 10^{-4}T^4 - 2.0672 \times 10^{-6}T^5)/100 \quad (6)$$

C_F makes it possible to assume a rough gradient of concentration at the melting plane $(\partial C/\partial y)_F$. The melting rate $\dot{m}_{mix}$ can be calculated by substituting C_F and $(\partial C/\partial y)_F$ into the mass balance of Eq. (5). Next, the $\dot{m}_{mix}$ $(= \dot{m}_{ice})$ is substituted into the heat balance of Eq. (4) to obtain a new value of T_F. If the new T_F is different from the old T_F, the iteration is continued until the new T_F coincides the old T_F which means a converged solution. As a result, the connection between Eqs. (4) and (5) makes it possible to determine the melting rate $\dot{m}_{ice}$, and also the temperature and concentration on the melting front T_F, C_F, which is of most concern for the melting of ice in mixtures.

A criterion iteration convergence was adopted as following.

$$\frac{|\phi^{n+1} - \phi^n|_{max}}{|\phi^{n+1}|_{max}} < \varepsilon_\phi \quad (7)$$

Moreover, another convergence tests such as time step, mesh size and relaxation factor were considered according to the method in the text of the SIMPLER, and also a bench mark test was conducted for the case of natural convection in a horizontal liquid layer [17]. Since the numerical solution will largely be dependent on the y-direction mesh size Δy due to the very complicated flow in the melt liquid and the very thin diffusion layer, it is necessary to set very small mesh sizes to obtain a precise numerical solution. In this calculations, variable mesh size was adopted in the y-direction, which increases gradually with a rate of 1.2 times until $i = 7$ (i.e. $\Delta y_{i+1} = 1.2\Delta y_i$). Especially, the effect of the most closest mesh size Δy_F on the melting rate was carefully considered as shown later. Eventually, the mesh size $\Delta y_F = 0.15$ mm was adopted in the present calculation. On the other hand, it was considered carefully the x-direction uniform mesh size Δx. Since the mean melting mass M calculated with $x = 0.67$ mm $(= L/150)$ was slightly larger, 2.4%, than that with $x =$ 1 mm $(= L/100)$, the uniform mesh size of $x = 1$ mm was adopted in the whole calculation domain in the melting system.

2.7. Definition of mean melting mass M and physical properties

Since the present study was mainly to focus on the mechanism of the melting and the melting rate during the comparatively short melting time (i.e. $t = 10$ min), the mean thickness of the melt layer was very small less than about 1.5 mm as will be seen later from the experimental results (Fig. 10). Therefore, it could be allowed that neglecting the movement of the melting front in the present numerical predictions would not prevent a resolution of the mechanism of melting. In other words, it is possible to predict the time evolution of the mean melting mass M from the $\dot{m}_{ice}$ predicted under the condition of a fixed melting front. However, the melting rate $\dot{m}_{ice}$ will change slightly and randomly along the horizontal direction as will be seen later. It is useful (or better) to define a mean melting mass M for practical applications as follows.

$$M = \int_0^t \left(\int_0^L \dot{m}_{ice}\, dx/L \right) dt \tag{8}$$

Table 1 shows the physical properties of $CaCl_2$ solution used in the present numerical predictions [18]. The thermal volumetric expansion β_T and the concentration volumetric expansion β_C were calculated from their definition by a least square approximation of the relation of density and temperature. Since it is difficult to find the mass diffusion coefficient D of a $CaCl_2$ aqueous solution for high concentrations and low temperatures which appeared in the present study, $D = 0.3 \times 10^{-9}$ m^2/s was adopted as a mean value of mixtures, because D for high concentration and low temperature had assumed to have a range of $0.1–0.5 \times 10^{-9}$ m^2/s as described in the previous report [13].

2.8. Concept of experimental procedure

All the experiments on the ice melting were conducted in a temperature controlled room below 0°C. The initial temperatures of the ice plate and liquid were arranged by adjusting the room temperature and the room temperature was maintained slightly below the initial temperature during the melting process.

Table 1
Physical properties of $CaCl_2$ aqueous solution for $T = -5$°C, $C = 0.2$ (20 wt%)

c_p (kJ/kg K)	3.044
Δh (kJ/kg)	334.1
β_C	−0.916
β_T (1/K)	0.00033
λ (kJ/m s K)	5.35×10^{-4}
μ (kg/m s)	0.00386
ρ (kg/m^3)	1193.9

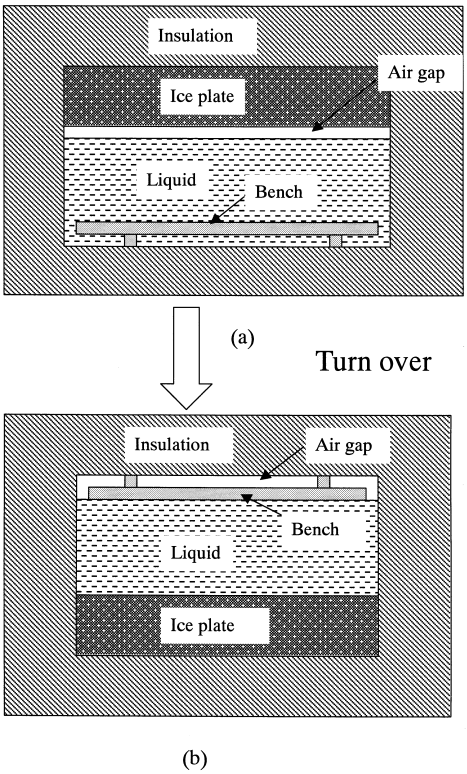

Fig. 3. The illustration of the concept of the melting experiment.

Fig. 3 shows an illustration of the concept of the experimental procedure. A new and special idea was proposed in the present experiment to fit the initial melting as closely as possible to the numerical procedure. A lucite plate bench was placed in the test cell as shown in Fig. 3(a), which was fixed on the bottom wall of the test cell. Liquid of the desired initial concentration of $C_i = 20$ wt% was poured in the test cell to the desired depth, and was maintained at the desired initial temperature of $T_{Li} = -5$°C. An ice plate with a desired thickness of δ was set on the top of the test cell and arranged so that no liquid leakage could occur when the test cell was inverted. After the temperature T_{Si} reached the temperature T_{Li}, the test cell was turned over gently so as not to disturb the liquid, and then an experimental run for the melting from above was started. The problem of volumetric change of the solid and liquid due to the phase change was not considered in this procedure.

The greatest difficulty in this experiment was to measure the temperature on the melting front T_F. It is difficult to measure T_F directly because of the steep gradient of temperature near the melting front. The temperature on the back surface of the ice plate T_1 (see Fig. 1) was measured to overcome this difficulty. Except in the early stage of melting, T_1 would be taken similar to T_F due to the larger thermal conductivity of ice compared to that of the liquid. Another temperature T_2 was also measured at a distance of $y =$ 15 mm from the initial melting front. All temperatures were automatically measured by using a personal computer with thermocouples during the melting time. After a desired time had passed, the ice plate was removed quickly from the test cell, and its weight was measured to determine the mean melting mass per unit area M. The aqueous solution of the desired initial concentration was made by weighing both water and $CaCl_2$ by using a precise balance with the sensitivity of 0.1 mg. Some complicated flows in the liquid were revealed by the technique of flow visualization using powder milk tracers.

3. Results and discussion

3.1. Consideration of mesh size

Fig. 4 shows the effect of mesh size Δy_F on the numerical results of the mean melting mass M and the minimum temperature in the melting system T_{min}. It can be seen that the results of both are stable in a range of Δy_F less than 0.2 mm. However, the melting rate (the minimum temperature) decreases (increases) considerably with increasing mesh size in the range larger than 0.2 mm. Therefore, it is desirable to use mesh sizes less than 0.2 mm for the melting of ice in aqueous solutions.

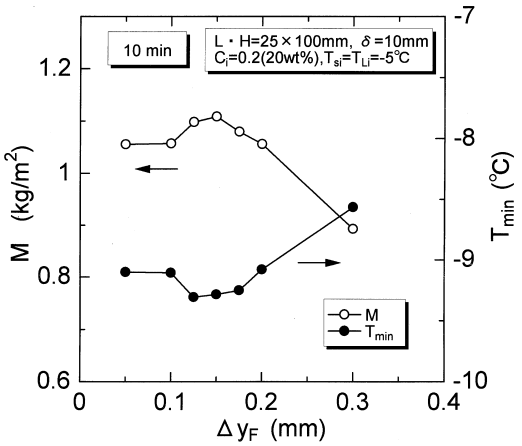

Fig. 4. Effect of mesh size Δy_F on the mean melting mass M and the minimum temperature decrease T_{min}.

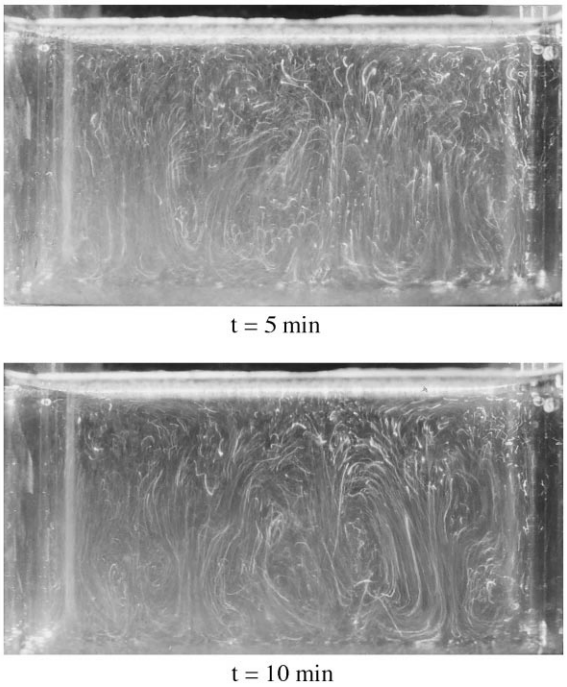

Fig. 5. Time evolution of flow observations in the liquid ($L = 100$ mm, $H = 50$ mm, $\delta = 20$ mm, $C_i = 20$ wt%, $T_{Si} = T_{Li} = -5°C$).

3.2. Flow in the liquid with visual observations and numerical predictions

Fig. 5 shows the visual observations of natural convection in the liquid, and Fig. 6 shows velocity vectors, isotherms, and isopleths of concentration. It is seen that very complicated large circulations and also small circulations in the melt liquid occur, which change during the melting process. The temperature near the melting front will decrease, which causes an increase in the liquid density, and therefore, will act to stabilize the liquid (negative buoyancy). On the other hand, the concentration near the melting front will decrease due to the adding of melt water, which causes a decrease in liquid density, and therefore, will act to make the liquid unstable (positive buoyancy). The predominance of the buoyancy due to density/concentration decrease causes many small spouts to appear near the melting front. It could be supposed that the connection of some spouts will cause a large plume to appear.

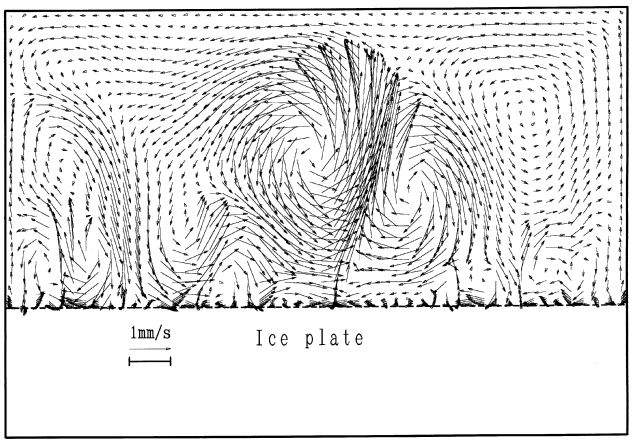

Velocity vectors

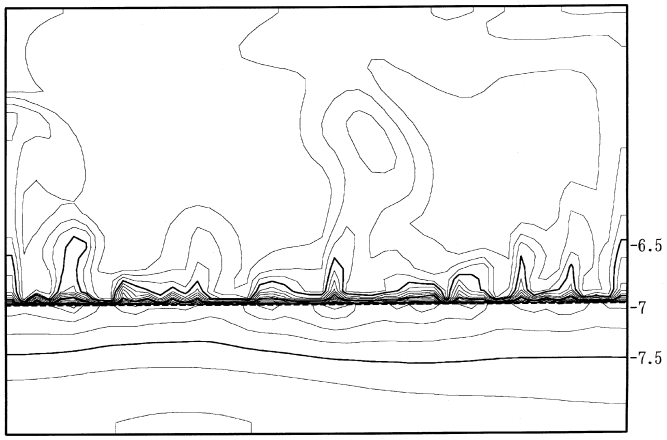

Isotherms (°C)

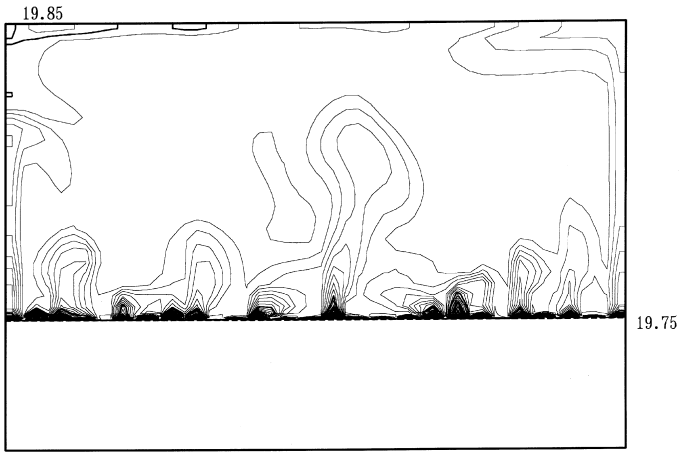

Concentration isopleths (wt%)

Fig. 6. Predicted results of velocity vectors, isotherms, and concentration isopleths at $t = 8$ min ($L = 100$ mm, $H = 50$ mm, $\delta = 20$ mm, $C_i = 20$ wt%, $T_{Si} = T_{Li} = -5°C$).

Although the flow patterns of visual and prediction do not agree exactly, the present two-dimensional numerical procedure predicts approximately the actual three-dimensional flow in the liquid.

Fig. 7 shows the predicted results for smaller liquid heights (a) $H = 15$ mm, and (b) $H = 25$ mm. The flow for the small liquid height is basically similar to the flow for the largest height of liquid $H = 50$ mm in Fig. 6. However, a typical difference is seen in that, the plumes for a small liquid height reaches directly to the top wall surface due to the strong inertia of the plumes.

3.3. Melting mass and decrease in temperature

Fig. 8 shows an example of the predictions for the melting rate $\dot{m}_{ice}$. It is seen that a wavy melting rate occurs, that is easily related to the flow vectors, isotherms, and isopleths of concentration in Fig. 7. The typical melting rate behavior can be understood more clearly from the horizontal temperature fluctuations in the liquid layer as shown in Fig. 9.

Fig. 10 shows comparisons of predictions and experiments for the mean melting mass and temperature decrease in the melting systems of (a) $H = 15$ mm and (b) $H = 25$ mm. The temperature T_1 at the bottom of the ice plate (see Fig. 1) decreases quickly from the initial temperature of -5°C just after the melting begins. Although the initial temperatures of both ice and liquid are the same -5°C as already explained, the temperature in the melting system will decrease spontaneously. This typical behavior seems curious; however, this will prove the fact of spontaneous melting of ice in an isothermal aqueous solution. The concentration gradient which appears near the melting front induces the melting of ice. At this time it is necessary to absorb the heat as latent heat for melting from ice and liquid, and therefore, a temperature gradient will appear on the melting front, and eventually, the temperature of the melting system will decrease spontaneously. The Lewis number Le is very large, about 400 in this problem. This means that the rate of mass

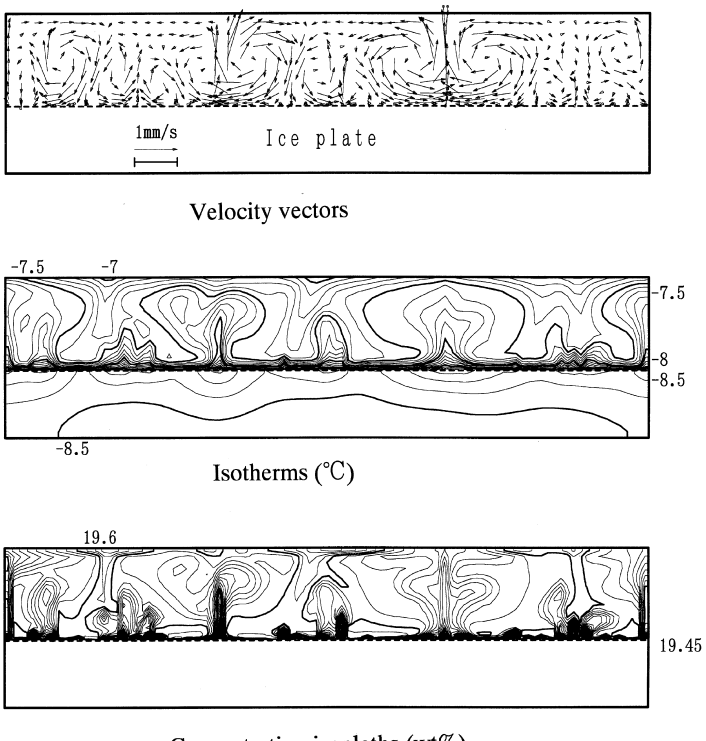

Fig. 7. Predicted results of velocity vectors, isotherms, and concentration isopleths for a small liquid heights at $t = 5$ min: (a) $H = 15$ mm, (b) $H = 25$ mm ($L = 100$ mm, $\delta = 10$ mm, $C_i = 20$ wt%, $T_{Si} = T_{Li} = -5$°C).

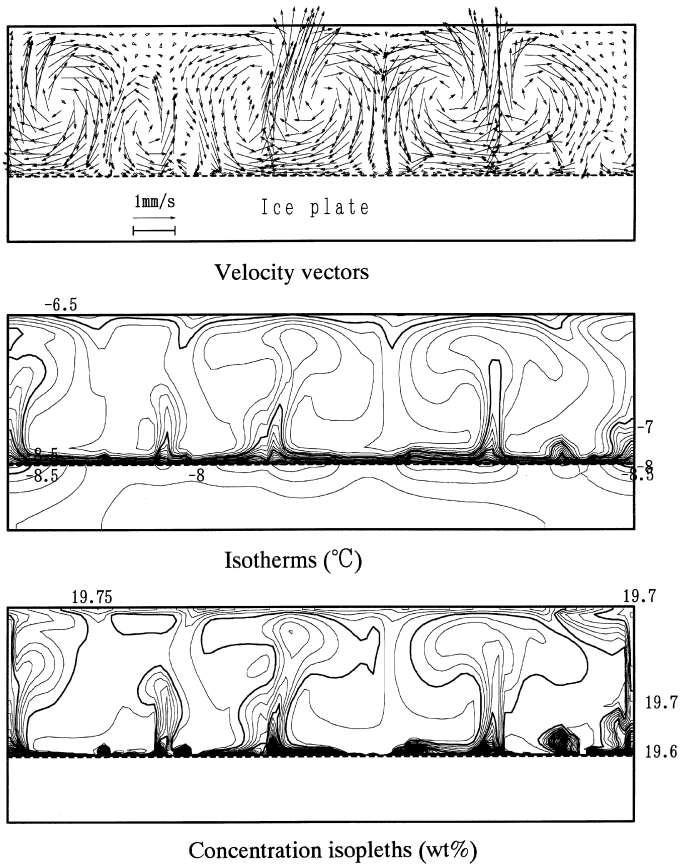

(b)

Fig. 7 (*continued*)

diffusion is very slow compared with the rate of heat conduction. Therefore, the melting of ice will be controlled by mass diffusion. The mean melting mass M will increase monotonically during the melting process.

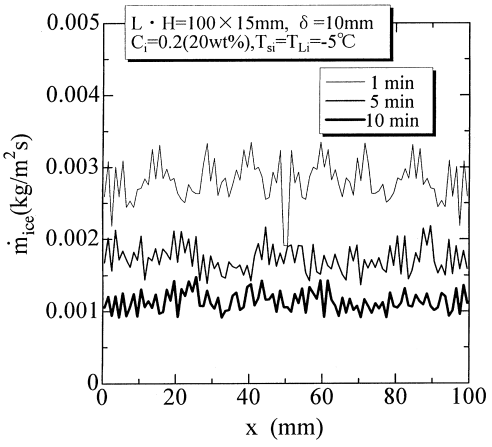

Fig. 8. Time evolution of the fluctuating melting rate $\dot{m}_{ice}$.

It is seen that M from the experiment is about 30% larger than predicted. This behavior is also reflected in the change of the ice temperature. At the present time,

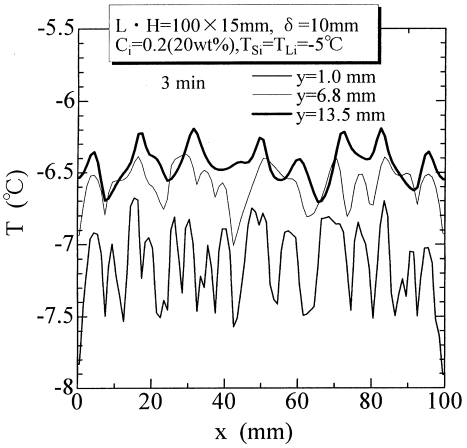

Fig. 9. Temperature fluctuation along the horizontal direction in the liquid.

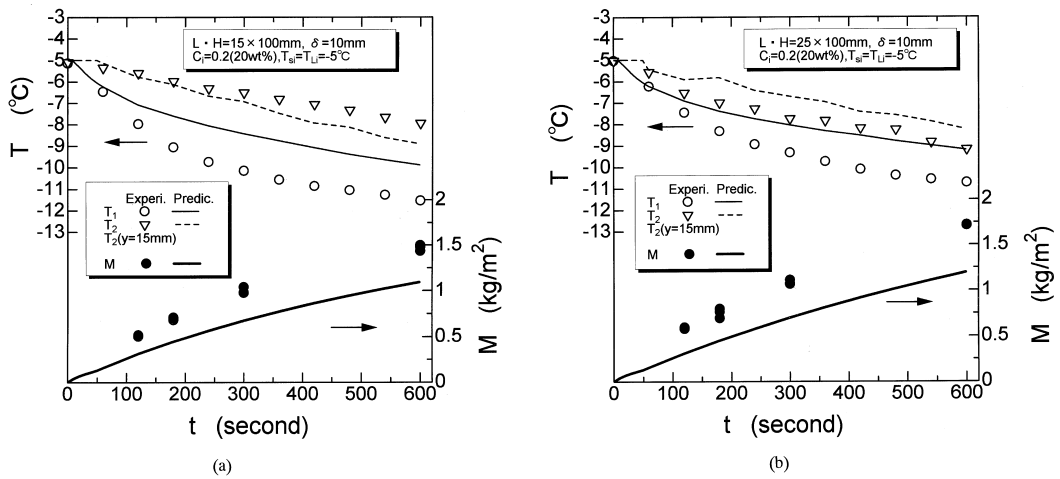

Fig. 10. Comparison of prediction and experiment for the temperature T_1, T_2 and the mean melting mass M: (a) $H = 15$ mm, (b) $H = 25$ mm.

it is difficult to explain exactly the discrepancy of experiment and prediction; however, it might be explained as follows. Fig. 11 shows a photograph of the melting front after an experiment. A very coarse surface is seen somewhat like *a sharkskin*, that could be the cause of promoting the melting mass of ice. However, it is very difficult to analyze such a very coarse surface. Another reason of the difference between experiment and prediction is considered to be the difference between a two-dimensional prediction

Fig. 11. Photograph of a very coarse melting front like a sharkskin.

and its ideal model and a three-dimensional experiment.

4. Concluding remarks

The melting of a horizontal ice layer from above in a $CaCl_2$ aqueous solution was considered experimentally and numerically. Summing up the results, the following can be concluded:

1. It was found out experimentally and numerically that very complicated flows appeared in the melt liquid, and changed randomly during the melting process.
2. A very coarse melting front was found after all experiments, that could play a key role in promoting the ice melting.
3. The present two-dimensional numerical calculations on an ideal model made it possible to predict approximately 30% less than the experimental results of the melting rate and the abrupt temperature decrease in the ice plate, which had not yet been previously reported.

Acknowledgements

Authors wish to acknowledge support for this study by the technical official T. Fujita and the under graduate students T. Okajima, A. Sawaki and M. Taguchi.

References

[1] O.M. Grifin, Heat, mass, and momentum transfer during the melting of glacial ice in sea water, ASME Journal of Heat Transfer 95 (1973) 317–323.
[2] E. Marschall, Free convection melting on glacial ice in saline water, Lett. Heat Mass Transfer 4 (1977) 381–384.
[3] H.E. Huppert, J.S. Turner, Ice blocks melting into a salinity gradient, J. Fluid Mech 100 (part 2) (1980) 367–384.
[4] E.G. Josberger, S. Martin, A laboratory and theoretical study of the boundary layer adjacent to a vertical melting ice wall in salt water, J. Fluid Mech 111 (1981) 439–473.
[5] V.P. Carey, B. Gebhart, Transport near a vertical ice surface melting in saline water, some numerical calculations, J. Fluid Mech 117 (1982) 379–402.
[6] V.P. Carey, B. Gebhart, Transport near a vertical ice surface melting in saline water, experiments at low salinities, J. Fluid Mech 117 (1982) 403–423.
[7] B. Sammakia, B. Gebhart, Transport near a vertical ice surface melting in water of various salinity levels, Int. J. Heat Mass Transfer 26 (1983) 1439–1452.
[8] R.S. Johnson, J.C. Mollendorf, Transport from a vertical ice surface melting in saline water, Int. J. Heat Mass Transfer 27 (1984) 1928–1932.
[9] M. Sugawara, H. Inaba, H. Nishimura, M. Mizuno, Melting of horizontal ice layer from above by combined effect of temperature and concentration of aqua-solvent, Wärme- und Stoffübertragung 21 (1987) 227–232.
[10] C. Beckermann, R. Viskanta, Double-diffusive convection due to melting, Int. J. Heat Mass Transfer 31 (1988) 2077–2089.
[11] S. Fukusako, M. Tago, M. Yamada, K. Kitayama, C. Watanabe, Melting heat transfer from a horizontal ice cylinder immersed in quiescent saline water, ASME Journal of Heat Transfer 114 (1992) 34–40.
[12] M. Sugawara, S. Sasaki, Melting of snow with double effect of temperature and concentration, ASME Journal of Heat Transfer 115 (1993) 771–775.
[13] M. Sugawara, T. Fujita, Melting of an ice layer with double effect of temperature and concentration (Second report, Development of numerical prediction with flow visualization), Trans. of JSME (Ser. B) 63 (1997) 2784–2792.
[14] E.R.G. Eckert, R.M. Drake, in: Analysis of Heat and Mass Transfer, McGraw-Hill, New York, 1972, pp. 718–719.
[15] S.V. Patankar, Numerical Heat Transfer and Fluid Flow, Hemisphere, Washington, DC, 1980.
[16] Japan Society of Mechanical Engineers, JSME Data Book: Thermo-physical Properties of Fluid (in Japanese), 1983, pp. 461–467.
[17] J.L. O'Tool, P.L. Silveston, Correlations of convective heat transfer in confined horizontal layers, Chemical Engineering Progress Symposium Series 57 (32) (1959) 81–86.
[18] Hand Book of Air Conditioning System Design (Part 4), McGraw-Hill, 1965, pp. 32–35.